Antivascular Therapy via Inhibition of Receptor Tyrosine Kinases in an Orthotopic Murine Model of Salivary Adenoid Cystic Carcinoma

Young-Wook Park, Hye-Jeong Kang, Jung-Min Park

Department of Oral and Maxillofacial Surgery, College of Dentistry, Kangnung National University, Korea

Abstract

Purpose: We evaluated the therapeutic effect of AEE788, a dual inhibitor of epidermal growth factor (EGF) and vascular endothelial growth factor (VEGF) receptor tyrosine kinases on human salivary adenoid cystic carcinoma (ACC) cells growing in nude mice.

Experimental Design: We examined the effects of AEE788 on salivary ACC cell growth and apoptosis. To determine the in vivo effects of AEE788, nude mice with orthotopic parotid tumors were randomized to receive oral AEE788 (50 mg/kg) three times per week, injected paclitaxel (200 μg) once per week, AEE788 plus paclitaxel, or placebo. Mechanisms of in vivo AEE788 activity were determined by immunohistochemical analysis.

Results: Treatment of salivary ACC cells with AEE788 led to growth inhibition and induction of apoptosis. AEE788 inhibited tumor growth and prevented lung metastasis in nude mice. Furthermore, AEE788 potentiated growth inhibition and apoptosis of ACC tumor cells mediated by paclitaxel. Tumors of mice treated with AEE788 and AEE788 plus paclitaxel exhibited down-regulation of activated EGFR and its downstream mediators (Akt and MAPK), increased tumor and endothelial cell apoptosis, and decreased microvessel density, which correlated with a decrease in the level of MMP-9, MMP-2 and bFGF expression and a decrease in the incidence of vascular metastasis.

Conclusions: These data show that tumor-associated endothelial cells are important in the process of tumor-metastasis. And VEGFR can be a molecular target for therapy of metastatic lung lesion of salivary ACC.

Key words

AEE788, Adenoid cystic carcinoma, Vascular metastasis, Molecular target

INTRODUCTION

Salivary adenoid cystic carcinoma (ACC) is one of the most common malignant tumors of parotid gland[1]. It is a slowly growing tumor, but sometimes it has a protracted clinical outcomes due to the invasion of the facial nerve, hematogenous metastasis without cervical nodal metastasis, and poor responses to classical chemotherapeutic agents[2]. Most deaths from salivary ACC are caused by vascular metastatic lesions[3]. Therefore the development of new treatment strategies for the recurrent metastatic lesions is a challenge. Especially knowledge of cellular properties and tumor-host interactions that influence the dissemination of metastatic cells is important for the design of more effective therapy of salivary ACC.

The epidermal growth factor receptor (EGFR) was known as the type I receptor tyrosine kinases, or ErbB receptors. This family is comprised of the EGFR (ErbB1/HER1), ErbB2 (HER2/neu), ErbB3 (HER3), and ErbB4 (HER4). EGFR is proposed as a major target for cancer treatment because it is overexpressed in a variety of epithelial tumors including salivary ACC[4-6]. And lots of evidence has accumulated that increased EGFR expression correlates with a poorer clinical results in a number of malignancies including head and neck squamous cell carcinoma[7]. In malignant tumor cells, EGFRs

* Corresponding author

Young-Wook Park
Dept. of OMFS, College of Dentistry, Kangnung National Univ.
Gangneung Daehangno 120, Gangneung, Gangwon-do, 210-702, South Korea
Tel: 82-33-640-3183 Fax: 82-33-640-3103
E-mail: ywpark@kangnung.ac.kr

※ This study was supported by a grant of the Korea Health 21 R&D Project, Ministry of Health & Welfare, Republic of Korea. (A060174)

can be activated in several mechnisms such as receptor overexpression[8-9], mutant forms of EGFR[10], or heterologous ligand-dependent mechanisms[11]. A main downstream signaling pathway of EGFR is via the Ras-Raf-MAP kinase (mitosis activated protein kinase, MAPK)[12], via phosphatidylinositol 3-kinase (PI3K) and the downstream protein-serine/threonine kinase Akt[13], or via the stress-activated protein kinase pathway, involving protein kinase C and Jak/Stat[14]. Activation of MAPKs regulates transcription of molecules that are linked to cell proliferation, survival, and transformation[15], and Akt transduces signals that trigger a cascade of responses from cell growth and proliferation to survival and motility[16]. These findings suggest that EGFR may play a key role in the progression and metastasis of certain types of epithelial tumors.

Tumor angiogenesis has been proposed as a critical step in oncogenesis and tumor metastasis. Various angiogenic and anti-angiogenic cytokines and pathways have been characterized. By targeting angiogenesis-related molecules, we can develop novel and minimally toxic anti-tumor treatments. However, few studies have examined the implications of expression of angiogenesis-related factors in salivary cancer. In 1996, investigators demonstrated that malignant salivary gland tumors overexpressed the mitogenic and angiogenic protein, fibroblast growth factor (FGF)-1, FGF-2 (basic FGF) and FGF receptor (FGFR)-1[17]. A recent study reported both vascular endothelial growth factor (VEGF) and basic FGF (bFGF) are major angiogenesis factors in salivary gland tumors[18]. And matrix metalloproteinase (MMP)-2, and MMP-9 were proposed as a invasion and metastasis-related factors in malignant tumors of salivary glands[19].

In our studies, angiogenic receptor, VEGFR-2 and angiogenic cytokines, IL-8 and MMP-9 are expressed at markedly higher levels in human salivary cancer xenografts[4]. And angiogenic signaling pathways are activated in clinical specimens of salivary ACC[20-21]. Moreover, VEGF, bFGF and MMP-9 have strong implications in vascular lung metastasis of orthotopic salivary tumor model[22]. Furthermore, microvessel density (MVD) is considered to be a prognostic indicator for the incidence of distant metastasis of salivary ACC[23]. These findings suggest that angiogenic signaling molecules have the potential of being therapeutic targets of salivary ACC.

Consistent with the above reviews, we hypothesized that activation of EGF-signaling pathway and angiogenic signaling pathway are critical for the progression and metastasis of human salivary ACC. Therefore their inhibition could be integrated into treatment options, especially for the management of metastatic lesions of salivary ACC. In the present study, we determined the therapeutic effect of a dual family EGFR/ErbB2 and VEGFR tyrosine kinase inhibitor, AEE788 (Novartis Pharma AG, Basel, Switzerland) against established ACC growing in the parotid glands of athymic mice. Because an anticyclic agents, paclitaxel is recently being evaluated in salivary cancer[24-25], we also evaluated the synergistic effect of AEE788 in combination with paclitaxel.

MATERIALS AND METHODS

Salivary Cancer Cells

A salivary cancer cell line, ACC3, was provided by Dr. Jeffrey N. Myers (Department of Head and Neck Surgery, University of Texas M.D. Anderson Cancer Center, Houston, TX, U.S.A.). These cells were maintained as monolayer cultures in RPMI-1640 medium containing 15% fetal calf serum, L-glutamine, vitamins (Life Technologies, Inc., Grand Island, NY), and penicillin-streptomycin (Flow Laboratories, Rockville, MD). The cells were incubated in a mixture of 5% CO_2 and 95% air at 37℃ The cultures were maintained for no longer than 12 weeks after recovery from frozen stocks.

Reagents

AEE788 which belongs to the class of the 7H-pyrrolo[2,3-d] pyrimidines was donated by Novartis Pharma Agency. Stock solutions (10 mM) of AEE788 were prepared in DMSO and stored at -20℃. Working solutions were prepared by diluting thawed stocks into cell culture medium. For *in vivo* administration, AEE788 was dissolved in 90% polyethylene glycol 300 + 10% 1-methyl-2-pyrrolidinone to a concentration of 6.25 mg/ml.

Paclitaxel was purchased from Sigma Chemical Co. (St. Louis, MO) and administered at 200 μg/week, a dosing regimen that was selected on the basis of results of previous studies at literature[26]. Propidium iodide (PI) and tetrazolium〔3-(4,5-dimethylthiazol-2-yl)-2,5-diphenyltetrazolium bromide; MTT〕were both purchased from Sigma Chemical Co.

Antibodies for immunohistochemical analysis were purchased as follows:

(1) rabbit polyclonal anti-EGFR (Santa Cruz Biotechnology);
(2) mouse rabbit polyclonal anti-phospho-AKT and anti-phospho-MAPK (Cell Signaling Technology);
(3) rabbit polyclonal anti-phospho-VEGFR-2 (Oncogene);
(4) rabbit polyclonal anti-MMP-9 and anti-MMP-2 (Chemicon) rabbit polyclonal anti-phospho-EGFR (Biosource International);
(5) rabbit polyclonal anti-bFGF (Sigma Chemical Co.)
(6) mouse anti-PCNA clone PC-10 (DAKO);
(7) monoclonal rat anti-CD31/PECAM-1 (PharMingen);
(8) peroxidase-conjugated goat anti-rabbit IgG (Jackson ImmunoResearch Laboratories);
(9) peroxidase-conjugated rat anti-mouse IgG2a (Serotec; Harlan Bioproducts for Science, Inc.);
(10) peroxidase-conjugated goat anti-rat IgG1 (Jackson Research Laboratories);
(11) Alexa Fluor 594-conjugated goat anti-rat IgG and Alexa Fluor 594-conjugated goat anti-rabbit IgG (Molecular Probes).

Other reagents for immunohistochemical analysis were ABC reagent (Biocare Medical), Hoechst dye 3342, MW 615.9 (Hoechst, Warrington), 3,3' -diaminobenzidine (DAB, Research Genetics), Gill' s hematoxylin (Sigma Chemical Co.), and pepsin (Biomeda). Terminal deoxyribonucleotidyl transferase-mediated dUTP nick end labeling (TUNEL) assay was performed using a commercial apoptosis detection kit (Promega Corp.).

In vitro Cytotoxicity Assay

Tumor cells (1×10^3) were seeded into 38-mm^2 wells of 96-well plates and allowed to adhere for 24 h. The cultures were then refed with medium with 2% serum.After 24 h,cells were treated with different concentrations of paclitaxel with or without AEE788 (negative control with DMEM alone). After a 72-h incubation, the metabolically active cells were determined by MTT assay. Briefly, after a 2-h incubation in medium containing 0.42 mg/ml MTT, the cells were lysed in dimethyl sulfoxide (DMSO). The conversion of MTT to formazan by metabolically active cells was measured using an MR-5000 96-well microtiter plate reader at an optical density of 570 nm (Dynatech, Inc.). Growth inhibition was calculated using the following formula: cytostasis (%) = [1-(A/B)] × 100, where A is the absorbance of treated cells and B is the absorbance of control cells.

In vitro Apoptosis Assay

Cells were plated at a density of 2×10^5 cells per well in a six-well plates . After a 24-h attachment period, the media were changed to 2% serum, and cells were maintained for 24 h and then treated with AEE788 and paclitaxel. After 72 h, both adherent and detached cells were harvested and washed with PBS and resuspended in PI, 50 μg/ml in 0.1% sodium citrate for 20 min at 4° C. Flow cytometric analysis was performed, and the percentage of apoptotic cells was calculated by gating the hypodiploid region on the DNA content histogram using Lysys software (BD, Franklin Lakes, NJ). The sub-G0/G1 fraction was used as a measure of the percentage of apoptotic cells. The percentage of cells undergoing specific apoptosis was calculated by subtracting the percentage of cells that had undergone spontaneous apoptosis in the relevant controls from the total percentage of apoptotic cells in the study cultures.

Evaluation of EGFR Mutations

To determine whether the salivary ACC cell line harbors EGFR mutations that might render it more sensitive to AEE788, polymerase chain reaction (PCR) was used to amplify exons 18, 19, and 21 from the human EGFR gene using genomic DNA isolated from ACC3 cells. The sequences of PCR primers are the same as the ones reported previously[27]. PCR amplicons were purified using QIAquick PCR purification kit (QIAGEN) and sent for sequencing. The sequencing results were then blasted and compared with the wild-type EGFR sequence from the Genebank.

Animals and Orthotopic Implantation of Tumor Cells

5-week old male athymic nude mice were purchased from the company (Orient Bio). The mice were used in accordance with the Animal Care and Use Guidelines of College of Dentistry, Kangnung National University. The mice used for this study were 6 weeks old.

To produce tumors, ACC3 cells were harvested from subconfluent cultures. The cells were resuspended in Ca^{2+}- and Mg^{2+}-free Hanks' balanced salt solution (HBSS). Only suspensions consisting of single cells with >90% viability were used for the injections. A total num-

ber of 1×10^6cells were resuspended in 30 μL of HBSS and injected into the parotid gland using a 27-gauge hypodermic needle and a 1ml-tuberculin syringe. A well-localized bleb confirmed a sussessful injection without leakage of the tumor cells. The preauricular incision was approximated in one layer using fine nylon sutures.

Treatment of Established Human Salivary Carcinomas Growing in the Parotid Glands of Nude Mice

Eight days after injection of the tumor cells, tumor nodules were palpable. Mice with similarly sized tumors were randomized into one of four groups (n=10 mice/group): group 1, the control group, received an oral diluent for AEE788 (90% polyethylene glycol 300 + 10% 1-methyl-2-pyrrolidinone) and i.p. HBSS group 2, the paclitaxel group, received paclitaxel by i.p. injection once per week (200 g/week); group 3, the AEE788 group, received AEE788 (50 mg/kg) by oral administration three times a week; and group 4, the combination therapy group, received both the i.p. paclitaxel regimen of group and the oral AEE788 regimen of group 3 concomitantly. Treatments continued for 7 weeks. Tumor size and body weight were measured once a week.

Necropsy Procedures and Histologic Examinations

Mice were euthanatized using carbon dioxide and their body weights were recorded. Primary tumors in the parotid glands were excised and weighed. For immunohistochemical and hematoxylin and eosin (H&E) staining, one part of the tumor tissue was fixed in formalin and embedded in paraffin. And another part was embedded in OCT compound (Miles Inc., Elkhart, IN), rapidly frozen in liquid nitrogen, and stored at -7℃. Cervical lymph nodes and lungs were harvested, and the presence of metastatic lesion was confirmed by histological review.

IHC Determination of EGFR/pEGFR, pAkt, pMAPK, MMP-9/MMP-2, bFGF and PCNA

Paraffin-embedded tissues were prepared for detection of EGFR/pEGFR, pMAPK, MMP-9/MMP-2, bFGF and PCNA. Frozen tissues were used for detection of pAkt. The tissues were sectioned at 8-10 μm, mounted on positively charged Plus slides and air-dried for 30 min. Sections were fixed in cold acetone (5 min), 1:1 acetone/chloroform (v/v; 5 min), and acetone (5 min) and then washed with PBS. For antigen retrieval, sections for pMAPK and PCNA were microwaved in 10mM sodium citrate buffer (pH 6.0; PCNA in water) for 5 min. And sections for bFGF were incubated in pepsin for 20 min at 37℃. Dilutions of primary antibodies were as follows: EGFR, 1:200; pEGFR, 1:25; pAkt, 1:100; pMAPK, 1:250; MMP-9, 1:50; MMP-2, 1:400; bFGF, 1:1,000; and PCNA, 1:100. Indirect peroxidase technique was used and positive reactions were visualized by incubating the slides with stable 3,3' -diaminobenzidine for 5 to 10 minutes. The sections were rinsed with distilled water, counterstained with Gill' s hematoxylin, and mounted with universal mounts.

Immunofluorescence Double Staining for CD31 and Phosphorylated VEGFR-2 or TUNEL

For TUNEL and double immunofluorescence assays, frozen tissues were used. After fixation with acetone, the samples were washed with PBS, incubated with protein-blocking solution containing 5% normal horse serum and 1% normal goat serum in PBS for 20 min, and then incubated with a 1:400 dilution of rat anti-mouse CD31 monoclonal antibody overnight at 4℃. After washing with PBS, the slides were incubated with a 1:600 dilution of secondary goat anti-rat antibody conjugated to Alexa Fluor 594 (red) for 1 h in the dark.

TUNEL assay was performed using an apoptosis detection kit with the following modifications. Samples were fixed with 4% paraformaldehyde for 10 min, washed twice with PBS for 5 min, and then incubated with 0.2% Triton X-100 for 15 min. After two 5-min washes with PBS, the samples were incubated with equilibration buffer for 10 min. The equilibration buffer was drained, and the reaction buffer, containing 44 μL of equilibration buffer, 5 μL of nucleotide mix, and 1 μL of terminal deoxynucleotidyl transferase (Promega Kit), was added to the sections and incubated in a humid atmosphere at 37C for 1 h, avoiding exposure to light. The reaction was terminated by immersing the samples in 2X SSC for 15 min. Samples were then washed with PBS to remove unincorporated fluorescein-dUTP.

Immunofluorescence double staining was performed by staining frozen samples with CD31. The samples were then incubated with primary antibody for anti-phospho-VEGFR-2 (1:400) overnight at 4C. After washing with

PBS, the samples were incubated with Alexa Fluor 594 (red)-conjugated secondary antibody for 1 h at room temperature. To identify the cell nuclei, the samples were incubated with 1 μg/mL Hoechst dye (Hoechst, Warrington) for 2 min. Immunofluorescence microscopy was performed in a Nikon Microphot-FXA (Nikon Inc., Garden City, NY) equipped with an HBO 100 mercury lamp, narrow bandpass filters to individually select for green, red and blue fluorescence (Chroma Technology Corp., Brattleboro, VT). Images were captured using a cooled CCD Hamamatsu 5810 camera (Hamamatsu Corp., Bridgewater, NJ) and Optimas Image Analysis software (Media Cybernetics, Silver Spring, MD). Photomontages were prepared using Adobe Photoshop software (Adobe Systems Inc., San Jose, CA).

Quantification of of PCNA, MVD, Absorbance, and Apoptotic Tumor and Endothelial Cells

For quantification analysis, five slides were prepared for each group and two areas were selected in each slide. To quantify PCNA and TUNEL expression, the number of positively stained cells and total cells were counted in 10 random 0.159-mm^2 fields of tumor area at $\times$100 magnification. The percentages of positively stained cells among the total number of cells were calculated and compared.

For the quantification of microvessel density (MVD), regions of high vascular density were identified by scanning the tumor sections at low microscopic power ($\times$40). The vessels that were completely stained with anti-CD31 antibodies were counted in 10 random 0.159-mm^2 fields at $\times$100 magnification.

For quantification of staining intensity, the absorbance of 100 MMP-9 and MMP-2 positive cells in 10 random 0.039-mm^2 fields at $\times$200 magnification taken from treated tumor tissues was measured using the Optimas Image Analysis software. The samples were not counterstained so that the absorbance would be attributable solely to the product of the immunohistochemical reaction. MMP-9 and MMP-2 cytoplasmic immunoreactivity was evaluated by computer-assisted image analysis and expressed as mean density value.

Quantification of apoptotic endothelial cells was expressed as the average of the ratiosof apoptotic endothelial cells to the total number of endothelial cells in 10 random 0.039-mm^2 fields at $\times$200 magnification.

Statistical Analysis

We calculated the dose and apoptosis rate using a Loess smoother, and 95% confidence intervals for the IC_{50} values using a parametric bootstrap methodology. For *in vivo* study, the Wilcoxon rank sum test was used to test for any difference in the tumor weight, body weight, and incidence of lung metastasis between the treatment and control groups. Quantitative analyses for the expression of PCNA, TUNEL, CD31, absorbance, and CD31/TUNEL were compared by unpaired Student's *t* test. For all analyses, a *P* value of less than 0.05 was considered statistically significant.

RESULTS

In vitro Cytotoxicity Mediated by AEE788 and Paclitaxel

To evaluate the effects of AEE788 on growth inhibition and an paclitaxel-induced cytotoxicity of human salivary cancer cells, ACC3 cells were incubated for 72 h in medium containing increasing concentrations (0-7 nM) of paclitaxel in the absence or presence of AEE788. When grown in media with 2% serum, growth of ACC3 cells was inhibited by AEE788 in dose-dependent manner, at IC_{50} of 4.3 μM. Furthermore, The IC_{50} of 3.4 nM for paclitaxel decreased to 2.6 and 0.9 nM when the cells were exposed to both paclitaxel and a noncytotoxic concentration of AEE788 (1.5 and 3 μM, Fig. 1). Therefore, the cytotoxicity mediated by paclitaxel was sensitizedby AEE788. But AEE788 did not increase the level of inhibition achieved with paclitaxel at higher concentrations.

In vitro Induction of Apoptosis by AEE788 and Paclitaxel

To assess the effects of AEE788 on the induction of apoptosis and on paclitaxel-induced apoptosis in human salivary cancer cells, ACC3 cells were incubated *in vitro* with paclitaxel in the absence of presence of AEE788 and then DNA fragmentation was quantified by flow cytometry with PI stanining. 72 hours after the start of treatment with AEE788, 50% of ACC3 cells were apoptotic at 8.2 μM (data not shown). Paclitaxel alone induced approximately 50% cell death at 5.9 nM, which was decreased to 3.5 nM and 2.3 nM by the addition of 2 μM and 4 μM AEE788, respectively (Fig. 2).

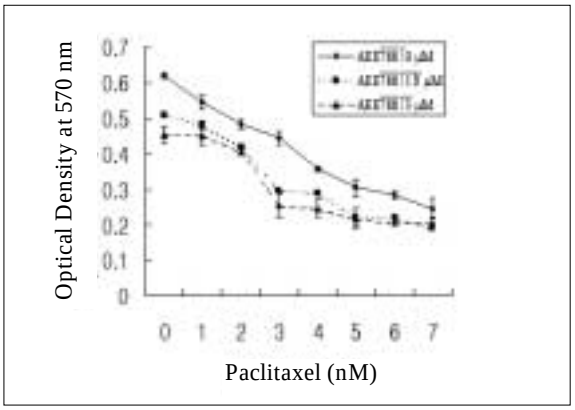

Fig. 1. Effect of AEE788 on paclitaxel-induced cytotoxicity. Cultured ACC3 cells were treated with paclitaxel (0-7 nM) with or without AEE788 at noncytostatic concentrations for 72 h, and the effect on cell growth was measured by MTT assay. The data were calculated as the mean ± SD of triplicate experiments.

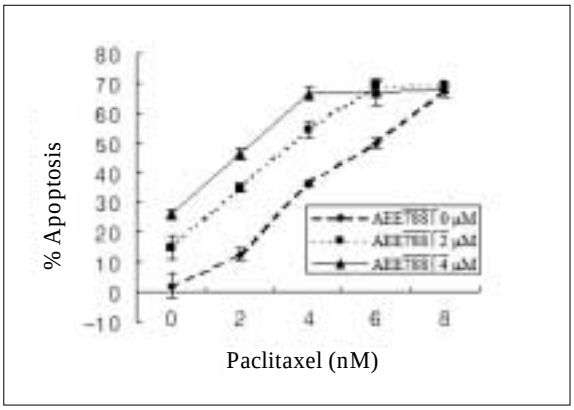

Fig. 2. Effect of AEE788 on paclitaxel-induced apoptosis. ACC3 cells were treated with paclitaxel (0-8 nM) with or without AEE788 (2, 4 μM) for 72 h, and the effect on the proportion percentage of cells undergoing apoptosis was determined by PI and flow cytometric assay. The data were calculated as the mean ± SD of triplicate experiments.

Table 1. *In vivo* effects of therapy with AEE788, paclitaxel, or both in human salivary ACC cells growing orthotopically in nude mice

Parameter	Treatment group[a]			
	Control	Paclitaxel	AEE788	AEE788 + Paclitaxel
Tumor weight, g				
Median	2.263	2.116	1. 570 [b]	0.853 [c]
Range	1.657-3.694	0.726-3.625	0.406-2.632	0.433-1.666
Incidence of cervical lymph node metastasis	0/10	0/10	0/10	0/10
Incidence of lung metastasis	5/10	2/10	0/10 [d]	1/10

[a] ACC3 cells (1×10^6) were injected into the parotid gland of nude mice. Eight days later, mice were randomized for treatment with once-weekly i.p. injections of paclitaxel (200 mg/week), three-times-weekly oral administration of AEE788 (50mg/kg), a combination of both drugs, or placebo as a control. All mice were euthanatized 7 weeks after initiation of therapy.

[b] $P < 0.05$ as compared with control (Wilcoxon non-parametric method).

[c] $P < 0.01$ as compared with control (Wilcoxon non-parametric method).

[d] $P < 0.05$ as compared with control (Fisher exact test).

PCR Analysis Demonstrates No EGFR Mutations

Sequence analysis revealed no mutations in exons 18, 19, and 21 of the EGFR gene in ACC3 cell line (data not shown).

Inhibition of Tumor Growth and Vascular Metastasis

To assess the effect of AEE788 on the *in vivo* growth of ACC3 cells, we used our murine orthotopic tumor model. After treatment of orthotopic parotid tumors, median parotid tumor weights (± SD) were 2.26±0.7g in controls and 2.12±0.91g in mice treated with paclitaxel. AEE788-treatment showed a significant reduction in

Table 2. Quantitative immunohistochemical analysis of ACC3 tumors in parotid glands of nude mice

Parameter	Treatment group[a]			
	Control	Paclitaxel	AEE788	AEE788 + Paclitaxel
Tumor cells, mean ± SD				
PCNA (%) [b]	61.8±4.4	50.8±7.5 [c]	20.9±6. 7 [c]	11.3±5.6 [c]
TUNEL (%) [b]	1.7±1.0	4.8±1.8 [c]	11.9±4.9 [c]	17.4±5.8 [c]
MMP-9 (OD) [d]	1.39±0.13	1.3±0.14	0.79±0.17 [c]	0.76±0.14 [c]
MMP-2 (OD) [d]	0.98±0.15	0.95±0.13	0.56±0.1 [c]	0.57±0.13 [c]
Endothelial cells, mean ± SD				
Microvessel density [e]	15.9±6.1	10.8±3.2 [f]	5.7±2.6 [c]	5.5±1.3 [c]
CD31/TUNEL (%) [g]	0	2.2±2.1 [c]	11.8±5.3 [c]	12.3±3.3 [c]

[a] ACC3 cells (1×10^6) were injected into the parotid glands of nude mice. Eight days later, mice were randomized for treatment with once-weekly intraperitoneal injections of paclitaxel (200 mg/week), three-times-weekly oral administration of AEE788 (50mg/kg), a combination of both drugs, or placebo as a control. Specimens were processed for immunohistochemical analyses 7 weeks after initiation of therapy.

[b] PCNA and TUNEL positivity was quantitated as the ratio of positively stained cells/total cells ×100 per field in 10 random 0.159-mm2 fields at ×100 magnification and 0.039-mm^2 fields at ×200 magnification.

[c] $P < 0.01$ as compared with controls (Wilcoxon non-parametric method).

[d] Absorbance determined as described in "Materials and Methods."

[e] Microvessel density was determined by measuring the number of completely stained blood vessels in 10 random 0.159-mm^2 fields at ×100 magnification.

[f] $P < 0.05$ as compared with controls (Wilcoxon non-parametric method).

[g] CD31/TUNEL positivity was quantitated as the ratio of CD31/TUNEL-positive cells/total endothelial cells × 100 in each of 10 random 0.039-mm^2 fields at ×200 magnification.

tumor weight (1.57±0.77g ; $P<0.05$). Moreover, the combination of AEE788 and paclitaxel demonstrated highly significant reduction in tumor weight (0.85±0.35g ; $P<0.01$). The median tumor weight of the combination treatment group was also compared with that of mice receiving AEE788 alone or paclitaxel alone. The difference in median tumor weight of paclitaxel-treated group ($P<0.01$) or AEE788-treated group ($P<0.05$) became statistically significant compared with combination treatment group.

We could not detect tumor cells in cervical lymph nodes. However, distant, hematogenous lung metastasis occurred in 5 of the 10 control mice, 2 of the 10 paclitaxel-treated mice, 0 of the 10 AEE788-treated mice, and 1 of the 10 mice in the combination therapy group. Our data suggested that both AEE788 and paclitaxel was able to prevent hematogenous metastasis to the lung compared with control ($P<0.05$, Table 1). AEE788 was well tolerated by the animals without significant side effects as determined by the maintenance of body weight (data not shown).

Effect of AEE788 on Salivary ACC in an Orthotopic Nude Mouse Model

Immunohistochemical analysis showed that tumors from mice in all four treatment groups expressed similar levels EGFR and its major downstream effectors (Akt and MAPK, data not shown). However, tumors from mice treated with AEE788 or the combination of AEE788 plus paclitaxel had decreased levels of activated EGFR, activated AKT, and activated MAPK compared with the control and paclitaxel-treated groups. Furthermore, tumors from mice treated with AEE788 or combination therapy had decreased PCNA levels, increased TUNEL-positive cells, and decreased expression of MMP-9, MMP-2 and bFGF, compared with the control (Fig. 3). Quantitatively, the mean percentage (±SD) of PCNA-positive (+) tumor cells in the control group was 61.8 ± 4.4. Compared with control, significant reduction ($P < 0.01$) in the percentage of PCNA+ tumor cells was detected in the paclitaxel-treated group (50.8 ± 7.5), AEE788-treated group (20.9 ± 6.7), and AEE788 plus paclitaxel-

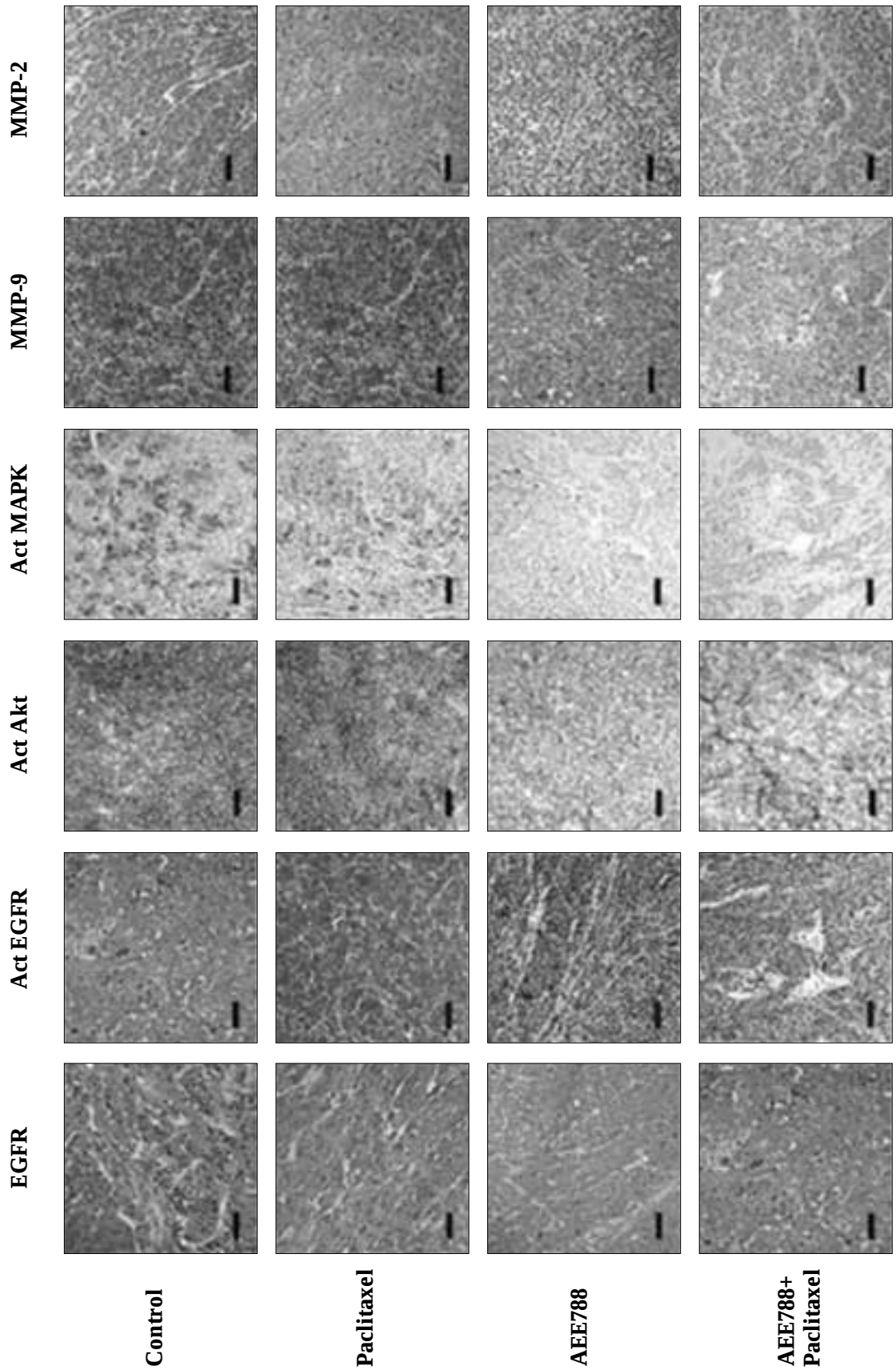

Fig. 3. Immunohistochemical analyses of ACC3 tumors harvested from control mice or mice treated with paclitaxel alone, AEE788 alone, or paclitaxel plus AEE788. The sections were immunostained for the expression of EGFR, activated (indicated as "Act") EGFR, activated Akt, activated MAPK, MMP-9 and MMP-2. Representative results are shown.

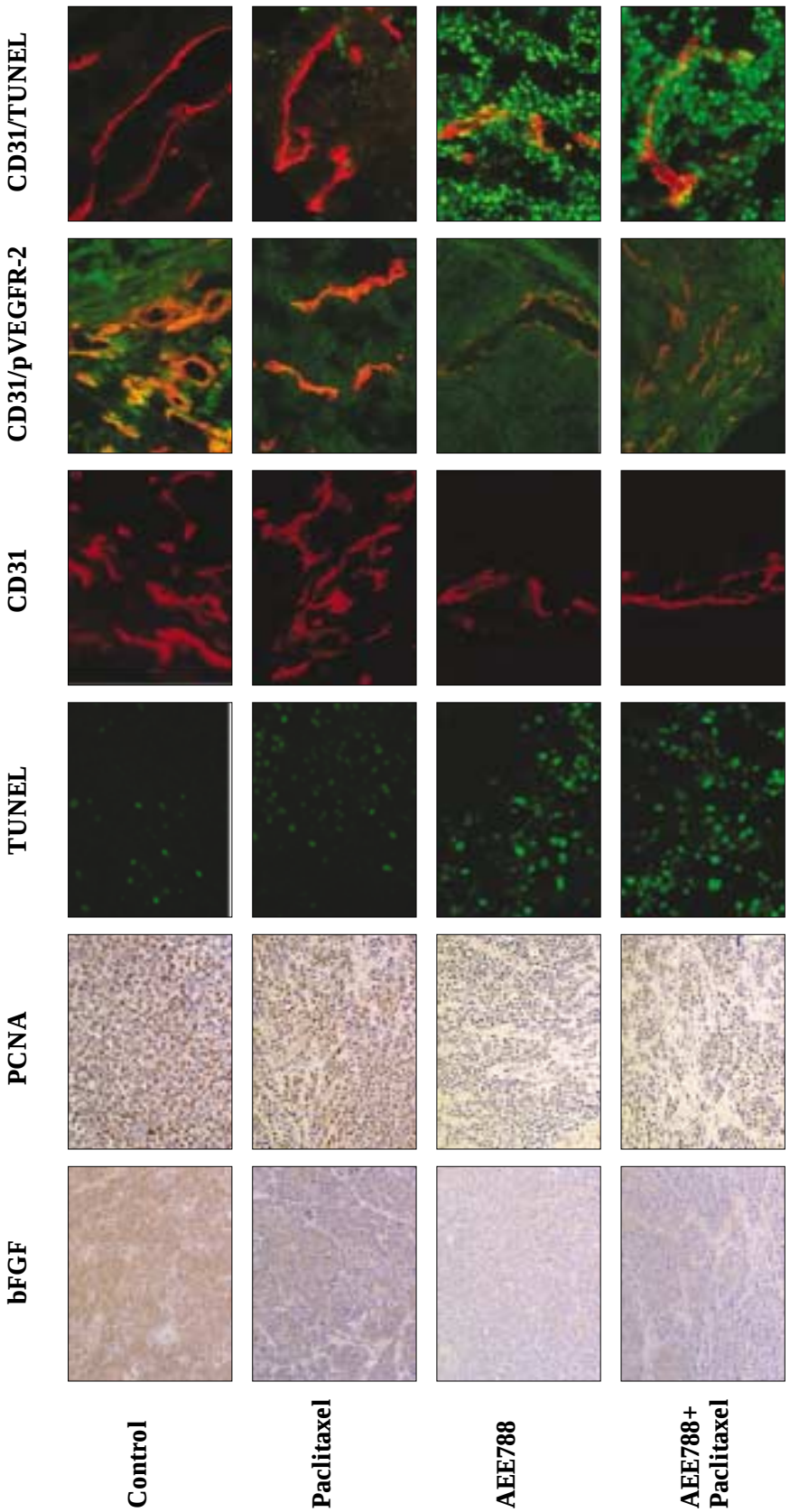

Fig. 4. Expression of bFGF (angiogenic factor), PCNA (tumor cell proliferation), TUNEL (tumor cell apoptosis), CD31 (endothelial cell marker), CD31/activated VEGFR-2 (activated endothelial cell), and CD31/TUNEL (endothelial cell apoptosis); Representative results are shown.

treated group (11.3 ± 5.6). The percentage of TUNEL+ cells in the control group was 5.1 ± 2.2. Compared with control, significant increase (P<0.01) in the percentage of PCNA+ tumor cells was detected in the paclitaxel-treated group (21.1 ± 7.4;), AEE788-treated group (40.3 ± 8.1), and AEE788 plus paclitaxel-treated group (57.4 ± 9.8). In addition, cytoplasmic immunoreactivity for MMP-9 and MMP-2 was significantly decreased after treatment with AEE788 and AEE788 plus paclitaxel, compared with control and paclitaxel-treated group (P<0.01, Table 2).

To evaluate the effect of AEE788 on the tumor-associated endothelial cells of ACC, immunohistochemical analysis was performed using antibodies against CD31, CD31/TUNEL, and CD31/pVEGFR-2. Tumors from mice treated with AEE788 or combination therapy demonstrated decreased MVD compared with the control. Quantitatively, the mean MVD was highest in the control group (15.9 ± 8.9). MVD was significantly decreased after treatment with paclitaxel (10.8 ± 3.2; P<0.05), AEE788 (5.7 ± 2.6; P<0.01), and AEE788 plus paclitaxel (5.5 ± 1.3; P<0.01). To detect apoptotic endothelial cells, double staining for CD31/TUNEL was performed with CD31 (red staining) and TUNEL (green staining). The percentage of CD31/TUNEL+ cells (yellow staining) was significantly increased in the tumors from mice treated with paclitaxel, AEE788, or AEE788 plus paclitaxel compared with control (P<0.01). However, there was no significant difference in MVD and the apoptotic endothelial cells after treatment with AEE788 plus paclitaxel, compared with AEE788-treated group. Double staining for CD31/activated VEGFR-2, which were performed with CD31 (red staining) and activated VEGFR-2 (green staining), revealed that only tumors from mice treated with AEE788 and AEE788 plus paclitaxel had decreased signal (yellow staining, Fig. 4).

DISCUSSION

Our results suggest that the tumor-associated endothelial cells within a primary salivary ACC can be a hopeful therapeutic target. We report that blockade of EGF and VEGF receptor tyrosine kinases by a small-molecular receptor tyrosine kinase inhibitor, AEE788 inhibits orthotopic tumor growth of salivary ACC and prevents lung metastasis in nude mice through induction of tumor and endothelial cell apoptosis. Furthermore, combination therapy of AEE788 (50 mg/kg, three times a week) plus paclitaxel (200 g/week) produces a synergistic therapeutic response resulting in a significant reduction in tumor growth and increase in tumor cell apoptosis. Our data also provide the experimental evidence for the essential role of MMP-9/MMP-2 and bFGF in neoangiogenesis and vascular metastasis of human salivary ACC.

In previous studies, we have identified that human salivary ACC expresses EGF and VEGF signaling proteins such as EGFR, HER-2, VEGFR-2 which can provide a survival and metastatic advantage of tumor cells by multiple mechanisms including increased angiogenesis[6,21]. We had also found in our preliminary study that EGFR and VEGFR-2 were present and phosphorylated in ACC3 cell line, determined by immunoblotting and immunohistochemistry[4]. Immunohistochemical staining of 18-20 clinical specimens of salivary ACC revealed that tumor-associated endothelial cells and stromal cells such as infiltrating inflammatory cells and tissue-specific fibroblasts as well as tumor cells were positive for expression of TGF-α, EGF, and VEGF[5,21]. These findings suggest that EGF and VEGF may play an important biologic role as a mitogen in autocrine manner and specific organ microenvironments play a key role in the progression of salivary ACC. Therefore, in addition to tumor cells, stromal cells associated with salivary ACC are potential targets against anti-EGFR/VEGFR strategies.

In the present study, we used the orthotopic murine model of parotid ACC, which was published in the previous report[28]. One of the striking features of salivary ACC is that metastases are usually hematogenous and most frequently involve the lungs. Lymph node metastases are uncommon and, when present, are more often the result of direct extension of the tumor into the lymph node rather than from embolic spread[29]. Our orthotopic parotid model of ACC exactly recapitulated the metastatic pattern of human tumors. Using this parotid tumor model, we could evaluate the effect of used small molecular inhibitor (AEE788) and a chemotherapeutic agent (paclitaxel).

In this study, AEE788, which is a reversible inhibitor of EGFR and VEGFR kinases, potently inhibits the receptor phosphorylation in ACC3 cells as proven in our Western blotting and immunohistochemical assays[4]. Furthermore, AEE788 inhibits phosphorylation of Akt and MAPK, which are downstream mediators of the EGF signaling pathways, relating to promotion of cellular proliferation and survival[30-31]. Treatment of salivary ACC cells, which had no EGFR mutations, with AEE788 led to dose-

dependent inhibition of cellular proliferation and induction of apoptosis. In addition, administration of AEE788 significantly reduced human salivary tumor growth in murine models. Moreover, this compound significantly inhibited tumor neoangiogenesis, resulting in inhibition of vascular metastasis to the lung.

The process of tumor metastasis are known to include the destruction of stroma and vascular basement membrane. The expression level of MMPs in certain malignant tumor system directly associated with invasion and metastasis[32-33]. Moreover, in mice that had received spleen cells from mice that expressed MMP-9, enhanced vascularity and tumorigenesis were associated with the expression of MMP-9 in macrophages, suggesting that tumor-infiltrating macrophages play an important role in the angiogenesis and growth of the human ovarian tumors in the animal model[34]. The extent of angiogenesis is determined by the balance between positive and negative regulatory factors, which are produced by tumor cells as well as by host stromal cells. Activated macrophages influence the tumor-associated neoangiogenesis by secreting enzymes that can break down the extracellular matrix and by secreting angiogenic factors and growth factors, such as bFGF, platelete-derived growth factor (PDGF), insulin-like growth factor-1, and VEGF/VPF[35-37]. Therefore, MMP and bFGF activity can enhance tumor growth and survival, invasion, angiogenesis and metastasis. In the present study, we demonstrated inhibition of the expression of MMP-9, MMP-2 and bFGF after treatment with AEE788, suggesting that the significant reduction in the incidence of lung metastasis was attributable to administration of AEE788.

Consistent with the above considerations, our immunohistochemical analysis suggests that inhibition of EGFR by AEE788 decreased Akt activity and subsequently decreased MMP-9 and MMP-2 production. As a result, intra-tumoral microvessel density (MVD) was decreased significantly and metastatic advantage was suppressed after treatment with AEE788. These data together with in vivo inhibition of VEGFR-2 phosphorylation of the tumor-associated endothelial cells, confirm the mechanism-based activity of AEE788 in our study.

Paclitaxel inhibits cell replication by enhancing polymerization of tubulin monomers into stabilized microtubule bundles that are unable to reorganize into the proper structures for mitosis and subsequent activation of apoptosis[38]. The antitumor activity of paclitaxel has been known to be potentiated by combination with EGFR tyrosine kinase inhibitors such as ZD1839 or PKI166[39-40]. A recent study reported that ZD1839 promoted paclitaxel-induced apoptosis of tumor cells by blocking paclitaxel-induced activation of the EGFR-ERK (extracellular signal-regulated kinase) antiapoptotic pathway[41]. Although anticyclic agents are not so effective on salivary tumors because the growth rate of salivary tumors is so slow, paclitaxel is currently being evaluated in salivary malignancies. In the present study, AEE788 inhibited in vivo growth of ACC xenografts in nude mice. However, the highest growth inhibition was achieved by concomitant administration of AEE788 and paclitaxel. In addition, our quantitative immunohistochemical analysis suggested that paclitaxel plus AEE788 revealed synergistic effects on the inhibition of tumor cell proliferation (PCNA positive) and induction of tumor cell apoptosis (TUNEL positive) compared with each single treatment group.

In summary, we have demonstrated that EGF receptors of tumor cells and VEGF receptors of tumor-associated endothelial cells are present in most of human salivary ACC. Blockade of EGFR and VEGFR signaling pathways by small molecular inhibitor has significant therapeutic effects on human salivary ACC cell xenografts in mice. The inhibition of *in vitro* and *in vivo* growth of tumor cells is mediated by both antitumor effects and antiangiogenic effects. Moreover, the antitumor effect of AEE788 was enhanced when it was combined with paclitaxel. Therefore, the antiangiogenic therapy via EGFR and VEGFR inhibition, is a valuable stratigy for the treatment of salivary ACC, warrnts clinical trials.

REFERENCES

1. Spiro RH: Salivary neoplasms, overview of a 35 year experience with 2,807 patients. Head Neck Surg 1986;8:177-184.
2. Fordice J, Kershaw C, El-Naggar A, Goepfert H: Adenoid cystic carcinoma of the head and neck: predictors of morbidity and mortality. Arch Otolaryngol Head Neck Surg 1999;125(2):149-152.
3. Teo PML, Chan ATC, Lee WY, Leung SF, Chan ESY, Mok CO: Failure patterns and factors affecting prognosis of salivary gland carcinoma: retrospective study. HKMJ 2000;6(1):29-36.
4. Park YW: Cellular and molecular characterization of adenoid cystic carcinoma of the salivary glands. J Kor Maxillofac Plast Reconst Surg 2005;27(2):110-122.
5. Park YW, Kim JH: Immunohistochemical assays for the expression of epidermal growth factor-signaling proteins in adenoid cystic carcinomas of human salivary glands. J Kor Maxillofac Plast Reconst Surg 2006;28(6):499-510.
6. Kim HS, Kim SM, Park YW: Immunohistochemical study on expression patterns of tumor growth related factors in salivary glands tumors. J Kor Maxillofac Plast Reconst Surg

2007;29(5):405-416.
7. O-charoenrat P, Rhys-Evans P, Modjtahedi H, Court W, Box G, Eccles S: Overexpression of epidermal growth factor receptor in human head and neck squamous carcinoma cell lines correlates with matrix metalloproteinase-9 expression and in vitro invasion. Int J Cancer 2000;86:307-317.
8. El-Rayes BF, LoRusso PM: Targeting the epidermal growth factor receptor. Br J Cancer 2004;91:418-424.
9. Khazaie K, Schirrmacher V, Lichtner RB: EGF receptor in neoplasia and metastasis. Cancer Metastasis Rev 1993;12:255-274.
10. Kuan CT, Wikstrand CJ, Bigner DD: EGF mutant receptor vlll as a molecular target in cancer therapy. Endocr Relat Cancer 2001;8:83-96.
11. Prenzel N, Zwick E, Daub H, Leserer M, Abraham R, Wallasch C et al: EGF receptor transactivation by G-protein-coupled receptors requires metalloproteinase cleavage of proHBEGF. Nature 1999;402:884-888.
12. Alroy I, Alroy I, Yarden Y: The ErbB signaling network in embryogenesis and oncogenesis: Signal diversification through combinatorial ligand-receptor interactions. FEBS Lett 1997;410:83-86.
13. Chan TO, Rittenhouse SE, Tsichlis PN: AKT/PKB and other D3 phosphoinositide-regulated kinases: Kinase activation by phosphoinositide-dependent phosphorylation. Annu Rev Biochem 1999;68:965-1014.
14. Yarden Y, Sliwkowski M: Untangling the ErbB signaling network. Nat Rev Mol Cell Biol 2001;2:127-137.
15. Lewis TS, Shapiro PS, Ahn NG: Signal transduction through MAP kinase cascades. Adv Cancer Res 1997;74:49-139.
16. Vivanco I, Sawyers CL: The phosphatidylinositol 3-Kinase-Akt pathway in human cancer. Nat Rev Cancer 2002;2:489-501.
17. Myoken Y, Myoken Y, Okamoto T, Sato JD, Kan M, McKEEHAN WL: Immunohistochemical study of overexpression of fibroblast growth Factor-1(FGT-1), FGT-2, and FGT Receptor-1 in human malignant salivary gland tumours. J Pathol 1996;178:429-436.
18. Ishibashi H, Shiratuchi T, Nakagawa K, Onimaru M, Sugiura T, Sueishi K et al: Hypoxia-induced angiogenesis of cultured human salivary gland carcinoma cells enhances vascular endothelial growth factor production and basic fibroblast growth factor release. Oral Oncol 2001;37(1):77-83.
19. Nagel H, Laskawi R, Wahlers A, Hemmerlein B: Expression of matrix metalloproteinases MMP-2, MMP-9 and their tissue inhibitors TIMP-1, -2, and -3 in benign and malignant tumours of the salivary gland. Histopathol 2004;44:222-231.
20. Park YW, In YS: Immunohistochemical assays for the expression of angiogenic signaling molecules and microvessel density in adenoid cystic carcinomas of human salivary glands. J Kor Oral Maxillofac Surg 2006;32(6):530-543.
21. In YS, Kim SM, Park YW: Comparative immunohistochemical assays for the expression of angiogenic factors in tumors of human salivary glands. J Kor Maxillofac Plast Reconst Surg 2007;29(1):10-23.
22. Jang JH, Kwon KJ, Park YW: Expressions of vascular metastasis related factors in murine orthotopic tumor models of salivary glands. J Kor Maxillofac Plast Reconst Surg 2007;29(6):499-508.
23. Yu F, Jiang XZ, Chen WT, Zhao YF, Zhou XJ: Microvessel density and expression of vascular endothelial growth factor in adenoid cystic carcinoma of salivary gland. Shanghai Kou Qiang Yi Xue 2003;12(6):443-446.
24. Perrot E, Davy N, Poubeau P, Arvin-Berod C: Chemotherapy with paclitaxel for lung metastases of cystic adenoidcarcinoma. A case report and review of the literature. Rev Pneumol Clin 2003;59(6):371-374.
25. Airoldi M, Fornari G, Pedani F, Marchionatti S, Gabriele P, Succo G: Paclitaxel and carboplatin for recurrent salivary gland malignancies. Anticancer Res 2000;20(5C):3781-3783.
26. Tedjarati S, Baker CH, Apte S, Huang S, Wolf JK, Killion JJ et al: Synergistic therapy of human ovarian carcinoma implanted orthotopically in nude mice by optimal biological dose of pegylated interferon alpha combined with paclitaxel. Clin Cancer Res 2002;8:2413-2422.
27. Lynch TJ, Bell DW, Sordella R, Gurubhagavatula S, Okimoto RA, Brannigan BW et al: Activating mutations in the epidermal growth factor receptor underlying responsiveness of non-small-cell lung cancer to gefitinib. N Engl J Med 2004;350:2129-2139.
28. Chung SH, Park YW: An experimental study for establishment of orthotopic salivary tumor models in mice. J Kor Oral Maxillofac Surg 2007;33(2):81-93.
29. Friedman EW, Schwartz AE: Diagnosis of salivary gland tumors. Cancer 1974;24:266-273.
30. Craven RJ, Lightfoot H, Cance WG: A decade of tyrosine kinases: from gene discovery to therapeutics. Surg Oncol 2003;12:39-49.
31. Castilla MA, Neria F, Renedo G, Pereira DS, González-Pacheco FR, Jiménez S et al: Tumor-induced endothelial cell activation: role of vascular endothelial growth factor. Am J Physiol Cell Physiol 2004;286(5):C1170-1176.
32. Chang C, Werb Z: The many faces of metalloproteases: cell growth, invasion, angiogenesis and metastasis. Trends in Cell Biol 2001;11(11):S37-43.
33. Bergers G, Brekken R, McMahon G, Vu TH, Itoh T, Tamaki K et al: Matrix metalloproteinase-9 triggers the angiogenic switch during carcinogenesis. Nat Cell Biol 2000;2:737-744.
34. Huang S, Van Arsdall M, Tedjarati S, McCarty M, Wu W, Langley R et al: Angiogenesis and progressive growth of human ovarian carcinoma is dependent on host metalloproteinase-9. J Natl Cancer (in press).
35. Koch AE, Polverini PJ, Kunkel SL, Harlow LA, DiPietro LA, Elner VM: Interleukin-8 as a macrophage derived mediator of angiogenesis. Science 1992;258:1798-1801.
36. Mantovani A, Bottazzi B, Colotta F, Sozzani S, Ruco L: The origin and function of tumor-associated macrophages. Immunol Today 1992;13:265-270.
37. Sunderkkotter C, Steinbrink K, Goebeler M, Bhardwag R, Sorg C: Macrophages and angiogenesis. J Leukoc Biol 1994;55:410-422.
38. Donaldson KL, Goolsby GL, Wahl AF: Cytotoxicity of the anticancer agents cisplatin and Taxol during cell proliferation and the cell cycle. Int J Cancer 1994;57:847-855.
39. Ciardiello F, Caputo R, Bianco R, Damiano V, Pomatico G, De Placido S et al: Antitumor effect and potentiation of cytotoxic drugs activity in human cancer cells by ZD-1839 (Iressa), an epidermal growth factor receptor-selective tyrosine kinase inhibitor. Clin Cancer Res 2000;6(5):2053-2063.
40. Holsinger FC, Doan DD, Jasser SA, Swan EA, Greenberg JS, Schiff BA et al: Epidermal growth factor receptor blockade potentiates apoptosis mediated by Paclitaxel and leads to prolonged survival in a murine model of oral cancer. Clin Cancer Res 2003;9(8):3183-3189.
41. Sumitomo M, Asano T, Asakuma J, Asano T, Horiguchi A, Hayakawa M: ZD1839 modulates paclitaxel response in renal cancer by blocking paclitaxel-induced activation of the epidermal growth factor receptor-extracellular signal-regulated kinase pathway. Clin Cancer Res 2004;10(2):794-801.